Covalently Modulated and Transiently Visible Writing: Rational Association of Two Extremes of Water Wettabilities

Supriya Das,[†] Ravi Kumar,[‡] Dibyangana Parbat,[†] Sylwia Sekula-Neuner,[‡] Michael Hirtz,[*,‡] and Uttam Manna[*,†]

[†]Department of Chemistry and Centre for Nanotechnology, Indian Institute of Technology Guwahati, Kamrup, Assam 781039, India

[‡]Institute of Nanotechnology (INT) & Karlsruhe Nano Micro Facility (KNMF), Karlsruhe Institute of Technology (KIT), Hermann von Helmholtz Platz 1, 76344 Eggenstein Leopoldshafen, Germany

ABSTRACT: Anticounterfeiting measures are of ever in creasing importance in society, e.g., for securing the authenticity of and the proof of origin for medical drugs. Here, an arms race of counterfeiters and valid manufacturers is taking place, resulting in the need of hard to forget, yet easy to read out marks. Anticounterfeiting measures based on micropatterns—while being attractive for their need in not widely available printing methods while still being easily read out with fairly common basic optical equipment—are often limited by being too easy to be destroyed by wear or handling. Here, nature inspired wettability is rationally exploited for developing an unprecedented anticounterfeiting method, where hidden information can be only identified under direct exposures to an aqueous phase or mist and disappears again on air drying the interface. A chemically reactive and hierarchically featured dip coating, capable of spatially selective covalent modification with primary amine containing small molecules, is developed for abrasion tolerant patterning interfaces with two extremes of water wettabilities, i.e., superhydrophilicity and superhydrophobicity. Arbitrary handwriting with glucamine followed by chemical modification with octadecylamine, provided "invisible" text on the synthesized interface. The glucamine treated region selectively becomes optically transparent and superhydrophilic due to rapid infiltration of the aqueous phase on exposure to liquid water or mist. The remaining interface remains opaque and superhydrophobic due to metastable entrapment of air. The hidden text became transiently and reversibly visible by the naked eye under exposure to liquid water/mist. Furthermore, microchannel cantilever spotting (μCS) is adopted for demonstrating well defined chemical patterning on the microscale. These patterns are at the same time highly resistant against wear and scratching because of the bulk functionalization, retaining the wetting properties (and thus pattern readout) even on serious abrasion. Such a simple synthesis of spatially controlled, direct, and covalently modulated wettability could be useful for various applied and fundamental contexts.

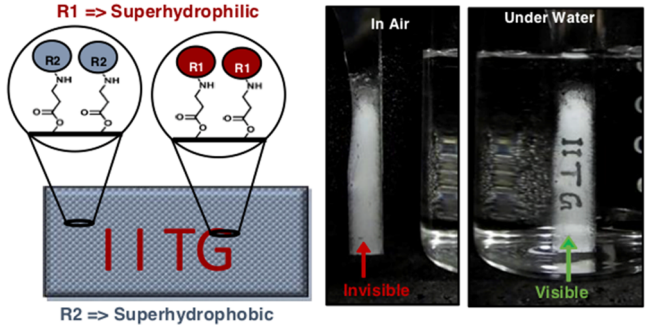

KEYWORDS: *superhydrophobicity, superhydrophilicity, chemically reactive, dip coating, anticounterfeiting*

INTRODUCTION

Hiding secret information is the general basis for defying the severe challenges related to counterfeiting.[1−8] Mostly, luminescence dependent approaches, including thermoplas monic nanoparticle, metal−organic frameworks, lanthanide based inks, complex wrinkling, etc.,[2−7] were adopted for this purpose. Moreover, hydrochromic dyes are strategically used in switching colors from invisible to visible depending on dry and wet conditions, where a change in molecular structure of the dye leads to a color change.[8] However, the inherent optical instability and uncontrolled quenching of the reported materials under repetitive exposures to day light and requirement of special equipment for identifying the hidden information are obvious existing challenges in the reported approaches. Therefore, further progress is essential for developing simple, but effective anticounterfeiting techniques.

Here, a covalent and spatially selective chemical modulation approach is unprecedentedly adopted for developing a luminescence free, transient, and reversible visualization of hidden information. This is achieved through the strategic use of two extreme water wettability properties: (1) super hydrophobicity[9,10] and (2) superhydrophilicity.[11,12] In the past, different biomimicked interfaces[9−12] were successfully exploited in demonstration of various practically relevant

potential applications, including oil/water separation, self cleaning, drug delivery, corrosion resistance, and so on.[13−25] In addition to this, different noncontact (UV light and laser assisted patterns) physical surface deposition[26−32] processes have been adopted for developing superhydrophobic and hydrophilic patterned interfaces, where the low surface chemistry of superhydrophobic coating is selectively compromised on top of the hierarchical interface.[26−32] Such synthetic designs are fundamentally inappropriate to sustain any practically relevant severe abrasive insults, and as expected, physically abraded interfaces completely failed to display any patterns. Moreover, examples of direct and contact based writing on superhydrophobic interface through the strategic use of chemical ink are rarely reported in the literature.

In the past, the concept of a hydrophobic/hydrophilic surface that can display a pattern through vapor condensation as a method to make counterfeiting is achieved with ultrathin self assembled monolayers (SAMs).[33] However, such interfaces are less likely to sustain under practically relevant physical abrasions. Here, using the current approach, a highly abrasion tolerant and chemically reactive porous polymeric coating is introduced for transiently visible writing. Such a demonstration is unprecedented in the literature, and such an approach could be useful for anticounterfeiting applications.

The metastable trapped air in the superhydrophobic material inhibits the infiltration of the aqueous phase in the hierarchically featured interface and provided heterogeneous and extreme aqueous repellency.[34] In contrast, superhydrophilic interfaces are highly water compatible and allowed rapid infiltration of the aqueous phase.[11] These distinct and extreme water wettabilities are associated with separate chemical requirements. There are very few reported approaches that are capable of modulating the chemistry in the hierarchically featured interfaces with (a) low surface energy and (b) high surface energy moieties. Earlier, our lab introduced chemically reactive multilayers (nine bilayers, each bilayer associated with six steps) of a polymeric nanocomplex for developing both superhydrophobicity in air and superoleophobicity under water from a single polymeric coating,[35] where the chemistry of the chemically reactive multilayers coatings is covalently modulated with appropriately selected small molecules. However, the synthesized polymeric coating was found to be inappropriate for spatially selective chemical modification as both organic and aqueous solutions of selected small molecules (glucamine) rapidly spread and spilled all over the interface; thus, developing a contact based, permanent pattern of two extreme liquid wettabilities was challenging.[35]

EXPERIMENTAL SECTION

Materials. Branched poly(ethyleneimine) (PEI, MW ∼ 25 000 g mol^{-1}), dipentaerythritol penta acrylate (5Acl, MW ∼ 524.21 g mol^{-1}), octadecylamine (ODA, 97%), sodium dodecyl sulfate (SDS), and dodecyl trimethylammonium bromide (DTAB) were obtained from Sigma Aldrich, Bangalore, India. 1 Heptanol (99%) was obtained from Alfa Aesar. Dimethyl sulfoxide (DMSO) was purchased from Thermo Fischer Scientific, Mumbai, India. Tetrahydrofuran (THF) was procured from RANKEM, Maharashtra, India. Microscopic glass slides were obtained from JSGW (Jain Scientific Glass Works, India). Dichloromethane (DCM) was acquired from Merck Life Science Pvt. Ltd., Mumbai, India. D Glucamine (>95%) and Nile Red (MW ∼ 318.38) were purchased from TCI (Tokyo Chemical Industry). Rhodamine 6 G and 1,2 dichloroethane (DCE, 98%) were acquired from LOBA Chemie (Laboratory Reagents and Fine Chemical) Mumbai, India, for experimental use.

General Characterization. The glass dipping vials were thoroughly washed with water, followed by acetone prior to preparing solutions of the respective chemicals. The glass slide (model substrate) was also thoroughly washed with methanol and deionized (DI) water. Contact angles and roll off angles of the beaded water droplets were measured on the material using the KRUSS Drop Shape analyzer DSA25 instrument with an automatic liquid dispenser at ambient temperature, and the dynamic water contact angles were measured at four different locations on each sample. A dynamic light scattering (DLS) study was performed using a Zetasizer Nano ZS90 instrument (model no. ZEN3690). All of the samples were coated with a thin layer of gold sputter prior to obtaining scanning electron microscopy (SEM) images of the thin layers using a Carl Zeiss field emission scanning electron microscope (FESEM). Fourier transform infrared (FTIR) spectra were acquired using a PerkinElmer spectrophotometer instrument at ambient temperature, where the polymeric matrix was mixed well with KBr prior to forming the KBr pellet. The digital images were captured by using a Canon Power Shot SX420 IS digital camera. The underwater optical transparency of the coating was measured using a PerkinElmer Lambda 750 (UV/vis/NIR spectrometer). The thickness of the coatings was measured using a Veeco Dektak 150 surface profilometer.

Preparation of the Reactive Thin Layer by Dip Coating. Solutions of 5Acl (265 mg mL^{-1}) and branched polyethylenimine (BPEI, 50 mg mL^{-1}) in 1 heptanol were prepared first in two separate glass vials. Then, 1.2 mL of BPEI was mixed with 4 mL of 5Acl solution in 1 heptanol to prepare reaction solution, and then a clean glass slide (5.5 cm × 1 cm) was taken as a model substrate and immersed into the solution immediately. The substrate was kept into the solution for different durations (e.g., 1, 3, 5, 7, 10 min). Next, the glass substrate was brought out from the reaction mixture and kept in air for drying. These polymeric dip coatings were thoroughly washed with THF, prior to postchemical modifications.

Postmodification with Desired Amine Containing Small Molecules. The chemically reactive polymeric coatings were covalently postfunctionalized with primary amine containing selected small molecules, including octadecylamine (5 mg mL^{-1}, in THF) and glucamine (2.5 mg mL^{-1}, in DMSO) following previously reported procedures. These chemically reactive polymeric dip coatings were exposed to a solution of amine containing small molecules. Next, the material was thoroughly washed with THF and dried under a stream of compressed air prior to further essential characterization or other relevant proof of concept experimental demonstrations.

Patterning on the "Reactive" Hydrophobic Thin Layer. For droplet based chemically modulated patterns, a couple of aqueous (alkaline, 10 μL) droplets of glucamine were gently placed on the inherently hydrophobic reactive polymeric coating for 5 min. Next, the beaded aqueous droplet was soaked with Kimwipes, and the whole substrate was kept in air for drying before exposure to a solution of octadecylamine (ODA, in THF). This spatially selective distinct chemical modulation allowed to develop patterned interfaces with two distinct liquid wettabilities (see text for more details). Next, the text was written with a fountain pen (Parker), where the ink was replaced with an aqueous solution of glucamine. After completion of manual writing, the selectively wetted interface was kept under a humid environment for 5 min, which helps in reducing the rate of evaporation of the aqueous phase. Next, the air dried interface was postmodified with ODA (in THF). This simple process provided invisible handwriting, which was only visible in the presence of mist or in contact with liquid water and became completely invisible again after air drying the patterned interface (see text for more details).

μCS Procedure. All patterning by μCS was done on the NLP 2000 instrument (Nanoink, Inc.). The microchannel cantilever[40,41] (SPT S C10S) was purchased from Bioforce Nanosciences. Prior to use, the microchannel cantilever was plasma cleaned by oxygen (0.2 mbar, 100 W, 20 sscm O_2, 2 min) on a Diener plama cleaning system Atto. The microchannel cantilever reservoir was then filled with 0.5 μL of ink, and the ink was pushed into the pen by blowing with a nitrogen stream. All patterning was done at room temperature, with different humidities, ranging from 50 to 70% RH. The STV cy3 and

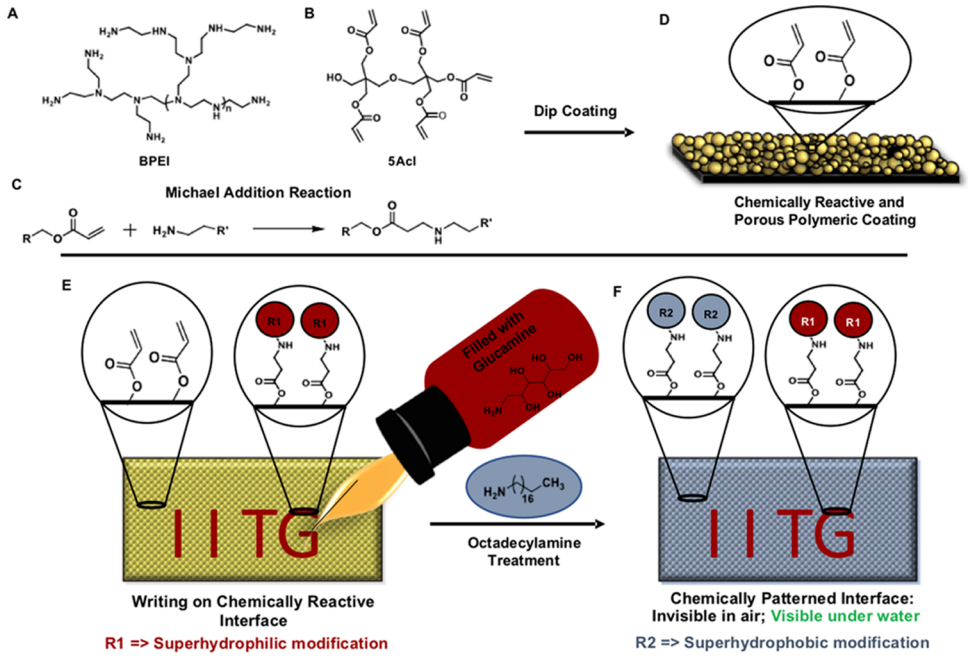

Figure 1. Chemical structures of branched polyethylenimine (BPEI), (A) and dipentaerythritol penta acrylate (5Acl, B), with (C) illustrating the Michael addition reaction between amine and acrylate groups. (D) Schematic presentation of chemically reactive polymeric dip coating that was directly prepared from the reaction mixture of BPEI/5Acl. Spatially selective chemical modulation of the amine reactive polymeric dip coating with aqueous ink of glucamine (E), followed by octadecylamine (F) for the synthesis of invisible patterns.

glycerol for producing the ink mixture were obtained from Sigma Aldrich (Germany). STV cy3 was used as received with a concentration of 1 μg μL^{-1}. After printing and resting time, the samples were washed with DI water (18.2 MΩ cm, Arium water system, Sartorius, Germany) to make sure to remove unbound ink. The samples were then dried with nitrogen before further analysis. All imaging was done on an upright fluorescence microscope (Eclipse 80i with DS Qi2 camera, Nikon Germany). The Supporting Information video was captured on in built software on a Nikon microscope.

RESULTS AND DISCUSSION

Here, a single step dip coating approach is introduced, making strategic use of the Michael addition reaction between branched polyethylenimine (BPEI) and dipentaerythritol penta acrylate (5Acl) as shown in Figure 1A–C.[36] The as synthesized amine reactive polymeric coating allowed (i) spatially selective postcovalent modification with glucamine, directly from an aqueous medium, as shown in Figure 1E, where a fountain pen filled with aqueous ink of glucamine was used to manually write "IITG". Furthermore, the postchemical modification with (ii) hydrophobic small molecules (octade cylamine, ODA; Figure 1F) yielded both invisible and permanent text. This hidden information was transiently and reversibly revealed on exposing the interface to either liquid water or even simply mouth's mist. We demonstrate the feasibility of micropatterning of these coatings by spotting microscale arrays showing the same wetting behavior on a much smaller scale.

Preparation and General Characterization of Coating. A transparent reaction solution of BPEI and 5Acl in heptanol rapidly transformed into an opaque solution due to the formation of the polymeric nanocomplex and eventually formed a semisolid polymeric gel within 15 min (Figure S1A). The size of the polymeric nanocomplex increases exponentially in the reaction mixture over time (Figure S1B). A cleaned glass slide was placed in this reaction mixture for a desired duration and removed from the reaction mixture followed by air drying. At the end, a polymeric coating is visible on the glass substrate; the thickness of the coating increases with longer immersion time (from 1 to 10 min) of the glass slide in the reaction mixture of BPEI/5Acl (Figure 2A). Further, water wettability was examined on the polymeric coatings that were prepared by varying the immersion time of the substrates in the reaction solution. The static water contact angle (SWCA) was gradually increased from ∼94 to ∼132° with increasing immersion time (from 1 to 10 min) of the respective substrate in the reaction solution, as noted in Figure 2A. This inherently high hydrophobicity helped in developing chemically modulated and spatially selective patterned interfaces that display a contrast in water (in air) or oil (under water) wettability, and such interfacial property is characterized in detail. Examining the topography of the synthesized polymeric coatings found that the morphology of the polymeric coatings significantly changed with increasing substrate immersion times in the reaction solution, as shown in Figure S2. A porous and hierarchical topography was noted in the polymeric coating that was prepared by immersing in the reaction solution for 10 min, where granular polymeric nanocomplexes were randomly aggregated and formed arbitrary microstructures, as shown in Figure 2B,C. Next, the available chemical functionality in the synthesized polymeric dip coating was examined by FTIR analysis. The appearance of IR peaks at 1410 and 1734 cm^{-1}, which were characteristic of (a) C–H stretching of β carbon of the vinyl groups and (b) carbonyl stretching, respectively,[36] revealed the existence of residual acrylate groups, as shown in Figure 2G. These unreacted acrylate groups were responsible for the reactivity of this polymeric dip coating toward amine molecules and provide a facile avenue for modulating chemistry in the synthesized material with desired chemical functionalities, as shown in Figure 2E,F. Next, samples of the chemically reactive polymeric dip coating were individually

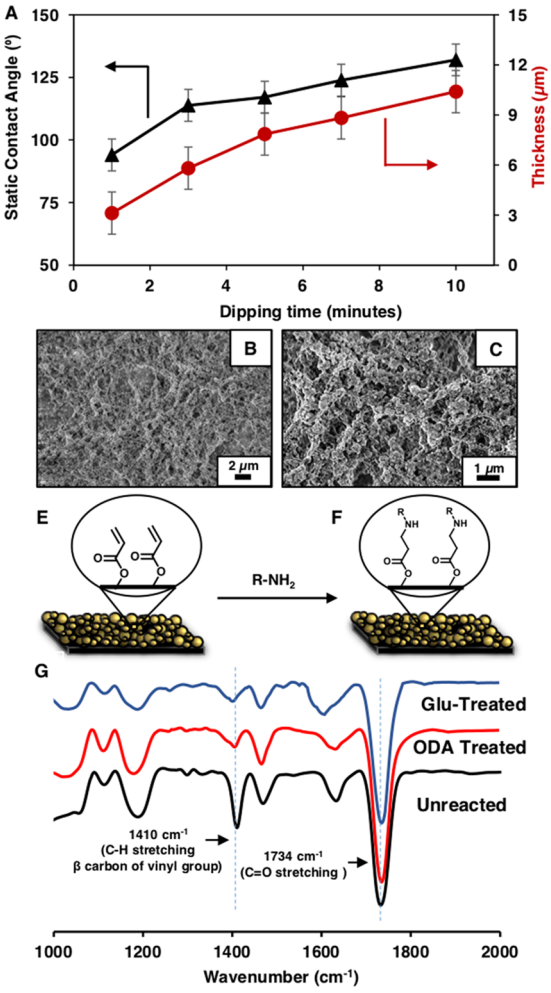

Figure 2. (A) Plot accounting for the change in the thickness and static water wettability of the polymeric dip coating—with the dipping time of the substrate in the reaction mixture of BPEI/5Acl. FESEM images of polymeric dip coating (after immersing in the reaction solution for 10 min) in low (B) and high (C) magnifications. (E, F) Schematic representation of postcovalent modulation of the as synthesized polymeric dip coating with primary amine containing small molecules through the Michael addition reaction. (G) FTIR spectra of chemically reactive dip coating before (black) and after postcovalent modulation with glucamine (blue) and octadecylamine (red).

treated with glucamine and ODA, and reinvestigated after chemical modification. The IR peak intensity at 1410 cm^{-1} that corresponded to the C−H stretching of the β carbon of the vinyl group was reduced significantly compared to the carbonyl stretching at 1734 cm^{-1} as internal reference shown in Figure 2G. During the Michael addition reaction, the carbonyl moiety in the residual acrylate groups remained unaffected, and the vinyl groups were converted from sp^2 hybridization to sp^3 hybridization on reaction with primary amine groups, as shown in Figure 2E,F. Thus, the IR peak intensity for C−H stretching of β carbon of the vinyl groups at 1410 cm^{-1} was reduced, which strongly suggests the successful covalent modulation of the chemically reactive polymeric dip coating with the primary amine containing small molecules.

Chemical Modulation of Wettability. Both the water (in air) and oil (under water) wettabilities were individually examined on chemically reactive polymeric coatings formed by dipping glass slides in the reaction mixture of BPEI/5Acl for different durations (1, 5, and 10 min), after chemical modification with ODA and glucamine, respectively. The inherently hydrophobic (static water contact angle ~136°) polymeric dip coating (prepared by 10 min of immersion in the reaction solution) became nonadhesive superhydrophobic with a static water contact angle of above 155° (Figure 3A−D) and a rolloff angle of 5°, as shown in Figure S3D−F. Water droplets instantly roll off on the ODA treated polymeric interfaces (see Supporting Movie 1), and a jet of water immediately bounces away after hitting the interface as shown in Figure S3. These simple demonstrations further revealed the nonadhesive superhydrophobicity. Moreover, this interface was found to be highly opaque (with transparency below 6% as shown in Figure S4) and shiny (Figure S3G, after inclining the interface) under water, due to the presence of metastable trapped air. This trapped external phase (air) is the primary element for minimizing the effective contact area between the water droplets and the synthesized superhydrophobic interface. The fraction of solid contact area with a liquid droplet can be estimated following general eqs 1 and 2

$$\cos\theta_r = f_1 \cos\theta - f_2 \quad (1)$$

$$f_1 + f_2 = 1 \quad (2)$$

where θ and θ_r are respective liquid (either water in air or oil phase under water) contact angles on both the smooth and featured interfaces, whereas f_1 and f_2 are defining the fraction of contact area between beaded liquid phase (water in air or oil under water) with solid interface and trapped external phase (air for superhydrophobic interface and aqueous phase for underwater superoleophobicity), respectively. To estimate the fraction of contact area, a smooth and featureless (as confirmed by FESEM imaging) polymeric coating was further developed using same chemicals (multilayer (nine bilayers) of BPEI/5Acl) but following a reported layer by layer deposition procedure.[27,28] The glucamine treated smooth coating displays a static oil contact angle (SOCA) of 106.5° under water, whereas the ODA treated multilayer was with a static water contact angle (SWCA) of 56.5° in air. Further, static water (in air) angles (see Figure 2A) on the ODA treated interfaces were used in eqs 1 and 2 for measuring the fraction of contact area between beaded water with metastable trapped air. Beaded water droplets (SWCA of 155.6°) remain mostly in contact with the metastable trapped air, and the fraction contact area was 0.943. Polymeric coatings formed with shorter immersion time (1 and 5 min) show adhesive superhydrophobicity after ODA treatment, where water droplets on such interfaces have an advancing water contact angle above 150° and contact angle hysteresis above 10°, as shown in Figure S3. The fraction of contact area between the metastable trapped air and the beaded water droplet was reduced to 0.87 (for 5 min) and 0.79 (for 1 min), respectively, allowing more interaction with the beaded liquid phase.

On the other hand, the same chemically reactive and inherently hydrophobic polymeric coating readily transformed to superhydrophilic in air with a water contact angle of 0°, after chemical modification with glucamine, as shown in Figure 3E,F. The hierarchically featured polymeric dip coating, being highly water compatible after glucamine treatment, was presumed to display fish scale inspired underwater super oleophobicity. As expected, the glucamine treated polymeric coating repelled the widely used model heavy oil (dichloro

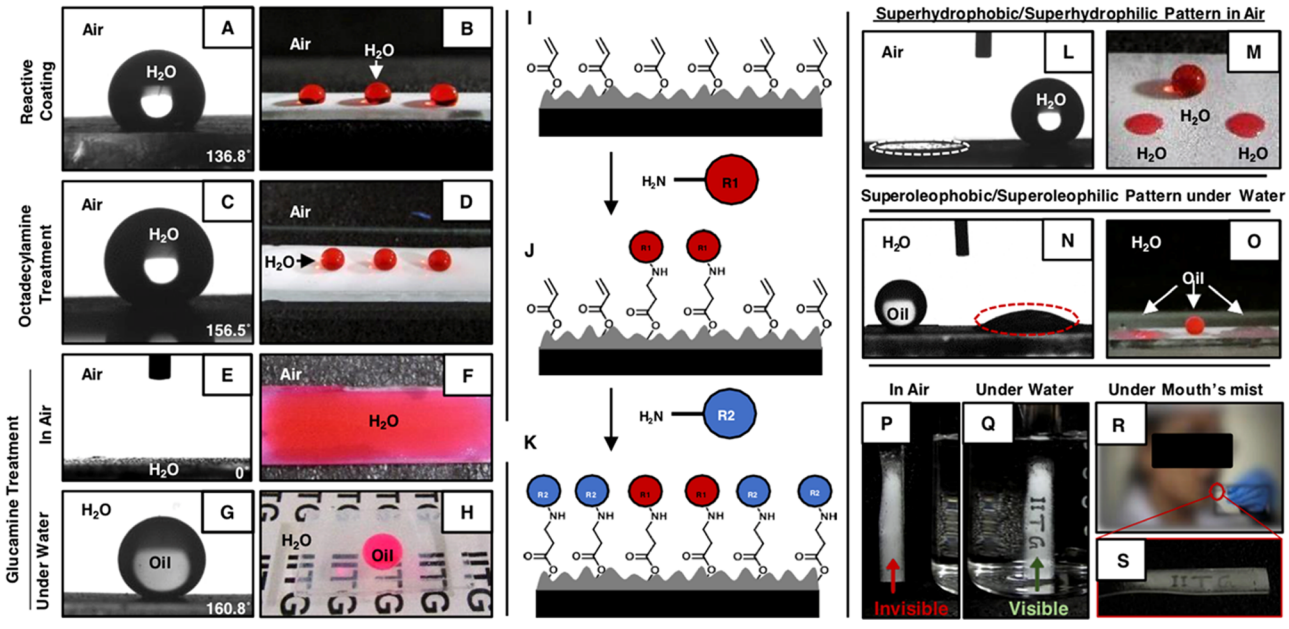

Figure 3. Contact angle (A, C, E, G) and digital (B, D, F, H) images of beaded water (in air; A–F) and oil (under water; G, H) droplets on the chemically reactive polymeric dip coating before and after treatments with octadecylamine (A–D) and glucamine (E–H). (I–K) Schematic representation of the location specific modulation of chemistry on the polymeric dip coatings with selected small molecules (J, K). Contact angles (L, N) and digital (M, O) images of location specific chemically modulated patterned interface that display superhydrophobic/superhydrophilicity (L, M; in air) and superoleophobicity/superoleophilicity (N, O; under water), where the bedding/spreading of water (in air) and oil (underwater) on glucamine and ODA treated area is demonstrated. The glucamine treated area in the patterned interfaces is indicated with the dotted white circles and the rest of the region is treated with ODA. (P, Q) Digital images of hand written (with glucamine loaded fountain pen) chemical pattern on the polymeric dip coating in air and under water; the hand written pattern is only visible under water, and the same pattern is invisible after air drying. (R, S) Digital image illustrating the effect of blowing moist air on the patterned interfaces; the hidden text is revealed after exposure to mouth mist (S).

ethane, DCE; colored with red dye) under water with a static oil contact angle of ~161.2° and a contact angle hysteresis below 10°, as shown in Figure 3G,H. The infused aqueous phase in the hierarchically featured polymeric dip coating (treated with glucamine) contributes to the extremely heterogeneous oil wettability under water by minimizing the contact area between the oil droplet and the polymeric dip coating. The fraction of solid interface that was exposed to the oil phase under water was calculated to be only 0.07, following the same eqs 1 and 2, as mentioned earlier. Moreover, this aqueous phase impregnated, extremely oil repellent polymeric dip coating (modified with glucamine) was found to be highly optically transparent (more than 80% under visible light (380–700 nm)) under water as shown in Figures 3H and S4.

Patterning of Coating and Abrasion Tests. The inherently hydrophobic and chemically reactive dip coating, capable of providing both superhydrophobicity and under water superoleophobicity (Figure S5), depending on the selection of appropriate chemical modifications, was further exploited in fabricating spatially selective and chemically controlled pattern, as shown in Figure 3I–K. Here, one type of chemical functionality was selectively applied in the desired location of the reactive dip coating before quenching the rest of the chemical functionality with another type of primary amine containing small molecules through a 1,4 conjugate addition reaction. This covalent bonding based backfilling approach allows us to fabricate arbitrary permanent patterns of two extreme and opposite liquid wettabilities, depending on the appropriate modification of the reactive dip coating with selected primary amine containing small molecules (glucamine, octylamine, octadecylamine, dopamine, etc.) or macromolecules (i.e., proteins). As a proof of concept demonstration, an alkaline (pH ~ 9) aqueous droplet of glucamine solution was placed on the chemically reactive and highly hydrophobic polymeric dip coating for spatially selective chemical modification of the coating with glucamine molecules. The rest of the residual acrylate groups in the polymeric coating were scavenged by reaction with a hydrophobic small molecule (ODA). This strategy yielded a superhydrophobic and superoleophobic patterned interface, where the glucamine treated regions were superhydrophilic, while the rest of the area was superhydrophobic, as shown in Figure 3L,M. Furthermore, oil wettability was examined on such chemically modulated patterned interfaces. Oil droplets instantly spread on ODA treated interfaces with a contact angle of 0°, while glucamine treated circular areas on the patterned interface repel oil under water extremely with a static oil contact angle of above 160°, as shown in Figure 3N–O. Thus, the described chemical modulation approach provides a single basis to create interfaces with patterned wettability within air (superhydrophobicity/superhydrophilicity) and under water (superoleophilicity/superoleophobicity). Furthermore, the synthesized chemically patterned superhydrophobic/superhydrophilic interface was exposed to an adhesive tape peeling test, which involves severe physical abrasion of the polymeric interfaces (Figure S6A–C). A freshly exposed adhesive tape was brought in contact with the chemically modulated patterned interface, and the top portion of the polymeric coating was arbitrarily cleaved and transferred to the adhesive surface during the peeling process, as shown in Figure S6C. However, the embedded patterned wettability remained unperturbed even after incurring such severe physical abrasion

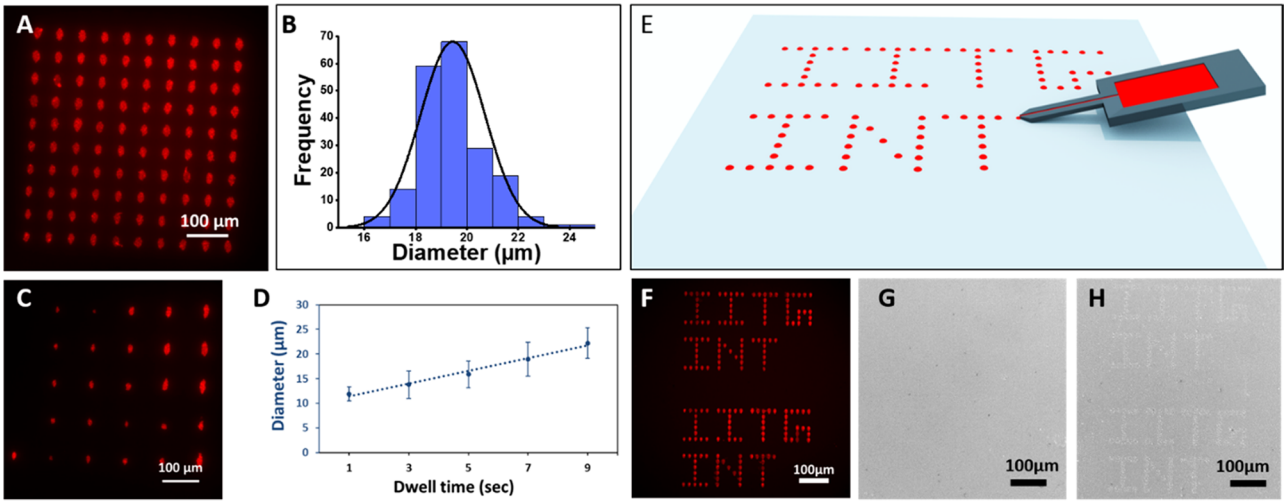

Figure 4. (A) Florescence microscopy image of a 10 × 10 dot microarray of a fluorescently labeled protein on amine reactive polymeric dip coating substrate after washing. The dots appear slightly elongated with respect to the cantilever orientation during μCS due to attachment of droplets to the cantilever by capillary forces. (B) Histogram derived from 200 features (two 10 × 10 dot microarrays as seen in (A)) showing the homogeneity of obtained patterns. (C) A 5 × 5 microarray written for probing different dwell times (columns from left to right where spotted with dwell times of 1, 3, 5, 7, and 9 s). The graph in (D) shows a linear dependence ($y = 2.59x + 8$) of average feature diameter with dwell time. (E) Scheme of μCS for IITG and INT microscale logos, spotted with a fluorescently labeled protein (F). Bright field images of a wettability pattern before (G) and during (H) exposure to humid air by breathing over the pattern.

to the polymeric coating, and a freshly exposed interior that transferred onto the adhesive tape is also capable of displaying contrast water wettability, as shown in Figure S6. Further, experiments were conducted to characterized postcovalent modification at the interior of the polymeric coating with glucamine through the 1,4 conjugate addition reaction. First, a large portion of the polymeric coating is modified with glucamine, and attenuated total reflection spectra were recorded before and after incurring adhesive tape peeling test on the same polymeric coating. The IR spectra are compared to chemically reactive polymeric coating for monitoring the covalent modification. Very similar depletion of IR peaks at 1410 cm^{-1} with respect to normalized IR peak for carbonyl stretching was noted before and after physical abrasion of the coating, as shown in Figure S6D. This IR analysis unambiguously revealed three dimensional postcovalent mod ification of porous polymeric coating with glucamine. Thus, this simple demonstration validated the existence of three dimensional nature of the chemically modulated pattern/ writing, which is capable of withstanding severe physical challenges, and examples of such designs are rarely reported in the literature. Such material could be useful in various potential applications. Here, this approach was extended further for covalently modulated apparently invisible handwriting—with contrast liquid wettability—for the first time, where the spatially selective displacement of trapped air allowed to control the transparency of the chemically modulated patterned interface depending on dry and wet conditions. The inherently hydrophobic and as synthesized highly chemi cally reactive hierarchical interfaces allowed to write text directly, without spreading or spilling, using a fountain pen loaded with an aqueous glucamine ink. Further, chemical modification with ODA provided permanent, invisible, and well defined text on such interfaces, with conceivable use for preventing counterfeiting. The apparently hidden (Figure 3P) information can be visualized by exposure to an aqueous phase, as shown in Figure 3R and Supporting Movie 2. As expected, this text disappeared again on the interface after air drying. Furthermore, this transient and reversible identification of the hidden information was also successfully achieved by exposing these patterned interfaces under mouth's mist (instead of direct exposure to liquid aqueous phase) for multiple (100) times, as shown in Figures 3R,S and S7J−M. In the past, the principle of breathing is widely and mostly used in developing different ordered porous films.[37] The invisible pattern on the polymeric coating became clearly visible in 99% humid air (Figure S8A,B). Moreover, the performance of the chemically patterned polymeric coating remained unaltered at both high (100 °C, Figure S9A,B, Supporting Movie 3) and low (10 °C, Figure S9C,D) temperatures. The same polymeric interface was contacted to a freshly exposed adhesive tape (Figure S9E), and during the peeling process, some top portion was physically abraded (Figure S9G). Nonetheless, the invisible pattern in the damaged interface was found to still be visible on exposure to water, as shown in Figure S9H,I. This impeccable durability of the chemically patterned interface is mostly due to the existence of three dimensional super liquid wettability in the polymeric coating, as evident from Figure S6. Thus, the strategic combination of contrast wettability and transparency provided a facile and completely different approach for easy and repetitive (100 times) identifications of invisible information, where the selective entrapment of metastable trapped air plays a crucial role. The same interface treated with ethanol, prior to exposure to water, is incapable of displaying hidden information, as shown in Figure S7F−I. As a further trial, this approach was extended to a model optically opaque substrate, i.e., filter paper. The same synthetic strategy was followed for creating a chemically modulated invisible patterned interface on the filter paper. The hidden information (in air) was revealed after transferring the coated filter paper in DI water (Figure S10A,B). Thus, the current approach is likely to be successfully generalized to various substrates.

Generation of Micropatterns. Anticounterfeiting can greatly benefit from miniaturization by the ability to hide a marking pattern to keep it secret until an authority needs to check authenticity and by making a marking pattern more

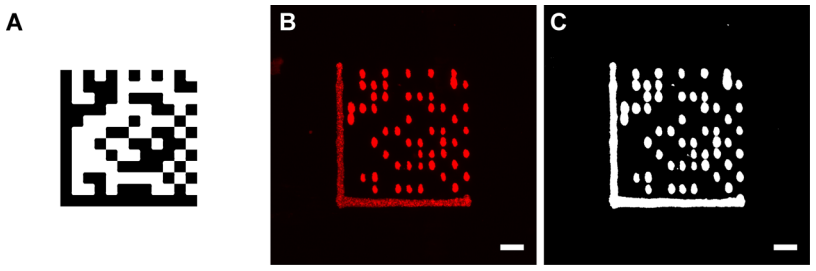

Figure 5. (A) Design pattern for a Data Matrix barcode encoding the acronym KNMF. (B) Fluorescence microscopy image of the 2D code printed via μCS. (C) Thresholded version of the image in (B) for better recognition by mobile phones. The scale bar equals 20 μm.

difficult to reproduce by counterfeiters with usually limited access to specialized micropatterning tools due to prohibitive investment costs and/or restriction in the sale of such machines. To elucidate the feasibility of miniaturizing the patterns on the coating and to show the effect of super hydrophobicity on the microscale, the microchannel cantilever spotting (μCS) technique was used to pattern dot microarrays under controlled environment and parameters.[38,39] First, for determining the pattern quality and establish writing parameters, streptavidin covalently bound with cyanine3 dye (STV Cy3) was spotted. The amine group in STV covalently binds to the amine reactive group on the surface and the cy3 dye can then be used to check the quality of the written pattern with fluorescence microscopy. The ink was admixed with 20 vol % glycerol for better flow of ink to the surface from cantilever and to prevent premature drying. A 10 × 10 dot array was patterned with a dwell time of 5 s at 60% relative humidity. To complete the reaction, samples were let at rest at room temperature overnight. Then, the samples were washed to remove excess ink and inspected (before and after washing) with bright field (BF) and fluorescence microscopy. The BF images show that no visible ink droplets remain on the surface after washing, but in fluorescence, the patterns are clearly visible after washing, which confirms successful immobilization of a thin film of protein (Figure S11). A typical outcome of such a spotting procedure is given in Figure 4 A. The feature size distribution measured over 200 features (from two 10 × 10 microarrays) gives an average diameter of 19.4 ± 1.3 μm (Figure 4B). The influence of reaction time was tested by washing the samples after different resting times and comparing the resulting fluorescence intensity (Figure S12). The binding reaction is obviously rather fast, as samples washed only minutes after patterning had shown no significant difference in fluorescence intensity after washing compared to samples that are allowed to rest for 1 h and longer. To establish further control over the patterning, a 5 × 5 matrix was patterned with different dwell times (1−9 s; Figure 4C). The obtained graph shows a linear dependence of average feature diameter with dwell time (Figure 3D). In addition to patterning dot features, also lines can be written with the cantilevers. Here, lines of 300 μm length were written with different speeds (1−50 μm s^{-1}), resulting in different line thicknesses, as more time is allowed for the ink to transfer when the cantilever is moved slowly (Figure S13). As examples of the arbitrary pattern shape, the IITG and "INT" logos were written (scheme shown in Figure 4E) with varying parameters (dwell time: 0.1−0.5 s, 45−60% RH); Figure 4E shows a typical fluorescence image after washing. The average feature diameter here is 13.5 ± 0.5 μm. Like before, the logos are not visible in BF after washing (Figure 4F). However, after exposure to humid air by breathing over the sample, the mist or vapor condensed on the pattern makes it visible for a few seconds (Figure 4G) before vanishing again when the humidity evaporates. This is especially obvious when dynamically observing the experiment during breathing over the pattern (Supporting Movie 4). Here, the effect of the streptavidin is similar to the glucamine for the macroscopic patterns, raising the local hydrophilicity of the surface in the patterned region and therefore enabling more condensation. Finally, to demonstrate one route for implementation of anticounterfeiting measures, a two dimensional (2D) barcode encoding the acronym "KNMF" based on the Data Matrix standard[42] was printed as fluorescent micropattern (Figure 5). In this way, serial numbers or other information can be encoded directly onto an item in a robust way.

CONCLUSIONS

In conclusion, we demonstrated a facile and chemically reactive dip coating allowing for tailoring surface liquid wettability through the selection of appropriate chemical modulations. The inherently hydrophobic and chemically reactive interfaces provided a facile basis for spatially selective covalent modification with utterly distinct functional molecules, yielding invisible chemical patterns. The handwriting with an aqueous ink of glucamine on the amine reactive interfaces, followed by octadecylamine treatment of the entire polymeric coating, provided invisible write up embedded within two distinct liquid wettabilities. The invisible write up became visible under direct exposure to liquid water or mouth mist. Furthermore, this coating allows for patterning in the microscale as we demonstrated by spotting experiments with μCS. Here, microarrays showing the same wetting and condensation behavior were demonstrated, showing the potential of the approach for miniaturized, invisible, but easy to reveal patterns. Such a simple and covalent modulation approach would be of potential interest for addressing issues related to anticounterfeiting and many other relevant challenges.

ASSOCIATED CONTENT

Supporting Information

The Supporting Information is available free of charge at https://pubs.acs.org/doi/10.1021/acsami.9b17470.

Digital image accounts and DLS study (Figure S1); FESEM images (Figure S2); contact angles (Figure S3); transmittance vs wavelength plot (Figure S4); static contact angles (Figure S5); digital images showing the retention of the circular hydrophilic pattern (Figures S6−S8, and S10); performance of an invisible chemically patterned interface (Figure S9); microscopic images

(Figure S11); fluorescence intensity comparison with different resting times (Figure S12); and line pattern (Figure S13) (PDF)

Demonstrations for nonadhesive superhydrophobicity (MOV)

Transient and reversible identification of the hidden information by exposure to an aqueous phase (MP4)

Performance of the chemically patterned polymeric coating at high and low temperatures (MP4)

Dynamic observation of the experiment during breathing over the pattern (MP4)

AUTHOR INFORMATION

Corresponding Authors

*E mail: michael.hirtz@kit.edu(M.H.).

*E mail: umanna@iitg.ac.in(U.M.).

ORCID

Michael Hirtz: 0000 0002 2647 5317

Author Contributions

The manuscript was written through contributions of all authors. All authors have given approval to the final version of the manuscript.

Notes

The authors declare no competing financial interest.

ACKNOWLEDGMENTS

The authors acknowledge financial support from Department of Biotechnology (DBT, India) (BT/PR21251/NNT/28/1067/2016), Ministry of Electronics and Information Technology (Grant no. 5(9)/2012 NANO), Department of Science and Board of Research in Nuclear Sciences (BRNS) (34/20/31/2016 BRNS, DAE YSRA), and Department of Atomic Energy (DAE). They thank CIF and Department of Chemistry, Indian Institute of Technology Guwahati, for their generous assistances in executing various experiments and for the infrastructures. U.M. acknowledges the DAAD Bilateral Exchange of Academics award (# 91727986). S.D. and D.P. are thankful to IIT G for their doctoral fellowships. This work was partly carried out with the support of the Karlsruhe Nano Micro Facility (KNMF, www.kmf.kit.edu), a Helmholtz Research Infrastructure at Karlsruhe Institute of Technology (KIT, www.kit.edu).

REFERENCES

(1) Auslander, J. D.; Berson, W. Bar Codes Using Luminescent Invisible Inks. Pitney Bowes U.S. Patent US5542971, 1996.

(2) Braeckmans, K.; De Smedt, S. C.; Roelant, C.; Leblans, M.; Pauwels, R.; Demeester, J. Encoding Microcarriers by Spatial Selective Photobleaching. *Nat. Mater.* **2003**, *2*, 169−173.

(3) Andres, J.; Hersch, R. D.; Moser, J. E.; Chauvin, A. S. A New Anti Counterfeiting Feature Relying on Invisible Luminescent Full Color Images Printed with Lanthanide Based Inks. *Adv. Funct. Mater.* **2014**, *24*, 5029−5036.

(4) Lee, J.; Bisso, P. W.; Srinivas, R. L.; Kim, J. J.; Swiston, A. J.; Doyle, P. S. Universal Process inert Encoding Architecture for Polymer Microparticles. *Nat. Mater.* **2014**, *13*, 524−529.

(5) Bae, H. J.; Bae, S.; Park, C.; Han, S.; Kim, J.; Kim, L. N.; Kim, K.; Song, S. H.; Park, W.; Kwon, S. Biomimetic Microfingerprints for Anti Counterfeiting Strategies. *Adv. Mater.* **2015**, *27*, 2083−2089.

(6) Jiang, Y.; Li, G.; Che, W.; Liu, Y.; Xu, B.; Shan, G.; Zhu, D.; Su, Z.; Bryce, M. R. A Neutral Dinuclear Ir(III) Complex for Anti Counterfeiting and Data Encryption. *Chem. Commun.* **2017**, *53*, 3022−3025.

(7) Kalytchuk, S.; Wang, Y.; Poláková, K.; Zbořil, R. Carbon Dot Fluorescence Lifetime Encoded Anti Counterfeiting. *ACS Appl. Mater. Interfaces* **2018**, *10*, 29902−29908.

(8) Sheng, L.; Li, M.; Zhu, S.; Li, H.; Xi, G.; Li, Y. G.; Wang, Y.; Li, Q.; Liang, S.; Zhong, K.; Zhang, S. X. A. Hydrochromic Molecular Switches for Water jet Rewritable Paper. *Nat. Commun.* **2014**, *5*, No. 3044.

(9) Feng, L.; Li, S. H.; Li, Y. S.; Li, H. J.; Zhang, L. J.; Zhai, J.; Song, Y. L.; Liu, B. Q.; Jiang, L.; Zhu, D. B. Super Hydrophobic Surfaces: From Natural to Artificial. *Adv. Mater.* **2002**, *14*, 1857−1860.

(10) Li, X. M.; Reinhoudt, D.; Crego Calama, M. What Do We Need for a Superhydrophobic Surface? A Review on the Recent Progress in the Preparation of Superhydrophobic Surfaces. *Chem. Soc. Rev.* **2007**, *36*, 1350−1368.

(11) Liu, M. J.; Wang, S. T.; Wei, Z. X.; Song, Y. L.; Jiang, L. Superoleophobic Surfaces: Bioinspired Design of a Superoleophobic and Low Adhesive Water/Solid Interface. *Adv. Mater.* **2009**, *21*, 665−669.

(12) Su, B.; Tian, Y.; Jiang, L. Bioinspired Interfaces with Superwettability: From Materials to Chemistry. *J. Am. Chem. Soc.* **2016**, *138*, 1727−1748.

(13) Chu, Z.; Feng, Y.; Seeger, S. Oil/Water Separation with Selective Superantiwetting/Superwetting Surface Materials. *Angew. Chem., Int. Ed.* **2015**, *54*, 2328−2338.

(14) Yao, X.; Gao, J.; Song, Y.; Jiang, L. Superoleophobic Surfaces with Controllable Oil Adhesion and Their Application in Oil Transportation. *Adv. Funct. Mater.* **2011**, *21*, 4270−4276.

(15) Kota, A. K.; Kwon, G.; Choi, W.; Mabry, J. M.; Tuteja, A. Hygo responsive Membranes for Effective Oil−water Separation. *Nat. Commun.* **2012**, *3*, No. 1025.

(16) Ueda, E.; Levkin, P. A. Emerging Applications of Super hyrophilic Superhydrophobic Micropatterns. *Adv. Mater.* **2013**, *25*, 1234−1247.

(17) To, M.; Xue, L.; Liu, F.; Jiang, L. An Intelligent Superetting PVDF Membrane Showing Switchable TransportPerformance for Oil/Water Separation. *Adv. Mater.* **2014**, *26*, 2943−2948.

(18) Wen, L.; Tian, Y.; Jiang, L. Bioinspired Super wettability from Fundamental Research to Practical Applications. *Angew. Chem., Int. Ed.* **2015**, *54*, 3387−3399.

(19) Cai, Y.; Lu, Q.; Guo, X.; Wang, S.; Qiao, J.; Jiang, L. Ultrasensitive and Broadband MoS_2 Photodetector Driven by Ferroelectrics. *Adv. Mater.* **2015**, *27*, 4162−4168.

(20) Gao, A.; Wu, Q.; Wang, D.; Ha, Y.; Chen, Z.; Yang, P. A Superhydrophobic Surface Templated by Protein Self Assembly and Emerging Application toward Protein Crystallization. *Adv. Mater.* **2016**, *28*, 579−587.

(21) Yu, C.; Cao, M.; Dong, Z.; Wang, J.; Li, K.; Jiang, L. Spontaneous and Directional Transportation of Gas Bubbles on Superhydrophobic Cones. *Adv. Funct. Mater.* **2016**, *26*, 3236−3243.

(22) Chen, K.; Zhou, S.; Wu, L. Self Healing Underwater Superoleophobic and Antibiofouling Coatings Based on the Assembly of Hierarchical Microgel Spheres. *ACS Nano* **2016**, *10*, 1386−1394.

(23) Wu, M.; Ma, B.; Pan, T.; Chen, S.; Sun, J. Silver Nanoparticle Colored Cotton Fabrics with Tunable Colors and Durable Antibacterial and Self Healing Superhydrophobic Properties. *Adv. Funct. Mater.* **2016**, *26*, 569−576.

(24) Yohe, S. T.; Freedman, J. D.; Falde, E. J.; Colson, Y. L.; Grinstaff, M. W. A Mechanistic Study of Wetting Superhydrophobic Porous 3D Meshes. *Adv. Funct. Mater.* **2013**, *23*, 3628−3637.

(25) Wang, J.; Kaplan, J. A.; Colson, Y. L.; Grinstaff, M. W. Stretch Induced Drug Delivery from Superhydrophobic Polymer Composites: Use of Crack Propagation Failure Modes for Controlling Release Rates. *Angew. Chem., Int. Ed.* **2016**, *55*, 2796−2800.

(26) Tadanaga, K.; Morinaga, J.; Matsuda, A.; Minami, T. Superhydrophobic−Superhydrophilic Micropatterning on Flowerlike Alumina Coating Film by the Sol−Gel Method. *Chem. Mater.* **2000**, *12*, 590−592.

(27) Geyer, F. L.; Ueda, E.; Liebel, U.; Grau, N.; Levkin, P. A. Superhydrophobic Superhydrophilic Micropatterning: Towards Ge

nome on a Chip Cell Microarrays. *Angew. Chem., Int. Ed.* **2011**, *50*, 8424−8427.
(28) Ueda, E.; Levkin, P. A. Emerging Applications of Superhydrophilic Superhydrophobic Micropatterns. *Adv. Mater.* **2013**, *25*, 1234−1247.
(29) Geng, H.; Bai, H.; Fan, Y.; Wang, S.; Ba, T.; Yu, C.; Cao, M.; Jiang, L. Unidirectional Water Delivery on a Superhydrophilic Surface with Two dimensional Asymmetrical Wettability Barriers. *Mater. Horiz.* **2018**, *5*, 303−308.
(30) Cao, M.; Li, Z.; Ma, H.; Geng, H.; Yu, C.; Jiang, L. Is Superhydrophobicity Equal to Underwater Superaerophilicity: Regulating the Gas Behavior on Superaerophilic Surface via Hydrophilic Defects. *ACS Appl. Mater. Interfaces* **2018**, *10*, 20995−21000.
(31) Kostal, E.; Stroj, S.; Kasemann, S.; Matylitsky, V.; Domke, M. Fabrication of Biomimetic Fog Collecting Superhydrophilic−Superhydrophobic Surface Micropatterns Using Femtosecond Lasers. *Langmuir* **2018**, *34*, 2933−2941.
(32) Si, Y.; Dong, Z.; Jiang, L. Bioinspired Designs of Superhydrophobic and Superhydrophilic Materials. *ACS Cent. Sci.* **2018**, *4*, 1102−1112.
(33) Du, X.; Wang, J.; Cui, H.; Tang, T.; Tianzhun, W. Vapor Condensation Assisted Reverse Display for Anti counterfeiting Applications. *Proc. IEEE* **2016**, 316−319.
(34) Cassie, A. B. D.; Baxter, S. Wettability of Porous Surfaces. *Trans. Faraday Soc.* **1944**, *40*, 546−551.
(35) Parbat, D.; Gaffar, S.; Rather, A. M.; Gupta, A.; Manna, U. A General and Facile Chemical Avenue for the Controlled and Extreme Regulation of Water Wettability in Air and Oil Wettability Under Water. *Chem. Sci.* **2017**, *8*, 6542−6554.
(36) Bechler, S. L.; Lynn, D. M. Reactive Polymer Multilayers Fabricated by Covalent Layer by layer Assembly: 1,4 Conjugate Addition based Approaches to the Design of Functional Biointerfaces. *Biomacromolecules* **2012**, *13*, 1523−1532.
(37) Zhang, A.; Bai, H.; Li, L. Breath Figure: A Nature Inspired Preparation Method for Ordered Porous Films. *Chem. Rev.* **2015**, *115*, 9801−9868.
(38) Hirtz, M.; Greiner, A. M.; Landmann, T.; Bastmeyer, M.; Fuchs, H. Click Chemistry Based Multi Component Microarrays by Quill Like Pens. *Adv. Mater. Interfaces* **2014**, *1*, No. 1300129.
(39) Atwater, J.; Mattes, D. S.; Streit, B.; von Bojničić Kninski, C.; Loeffler, F. F.; Breitling, F.; Fuchs, H.; Hirtz, M. Combinatorial Synthesis of Macromolecular Arrays by Microchannel Cantilever Spotting (μCS). *Adv. Mater.* **2018**, *30*, No. 1801632.
(40) Xu, J.; Lynch, M.; Huff, J. L.; Mosher, C.; Vengasandra, S.; Ding, G.; Henderson, E. Label Free Protein and Pathogen Detection Using the Atomic Force Microscope. *Biomed. Microdevices* **2004**, *6*, 117−123.
(41) Xu, J.; Lynch, M.; Nettikadan, S.; Mosher, C.; Vegasandra, S.; Henderson, E. Microfabricated "Biomolecular Ink Cartridges"—Surface Patterning Tools (SPTs) for the Printing of Multiplexed Biomolecular Arrays. *Sens. Actuators, B* **2006**, *113*, 1034−1041.
(42) *GS1 DataMatrix Guideline, Release 2.5.1*, Ratified, Jan 2018. https://www.gs1.org/docs/barcodes/GS1 DataMatrix Guideline.pdf, accessed Nov 19, 2019.